Journal of Solar Energy Research (JSER)

Journal homepage: jser.ut.ac.ir

Assessment of wet compression integrated with air-film blade cooling in gas turbine power plants

Hassan Athari [a,*], Mostafa Delpisheh [b], Maghsoud Abdollahi Haghghi [a,c,**], Yusef Rahimi [a]

[a] *Department of Mechanical Engineering, Elm-o-Fann University College of Science and Technology, Urmia, Iran*
[b] *School of Mechanical Engineering, Iran University of Science and Technology (IUST), Tehran, Iran*
[c] *Department of Mechanical Engineering, School of Engineering, Urmia University, Urmia, Iran*

Received: 2021-07-01
Accepted: 2021-08-10

Abstract

The output power, energy, and exergy efficiencies of gas turbines significantly decrease by rising ambient temperatures during warm weather periods. The utilization of evaporative inlet cooling in gas turbine cycles increases its performance, which is extremely useful when trying to meet the increasing electrical power demands and offsetting shortages during peak load times, especially in these warm periods. With this in mind, the present study focuses on the thermodynamics of a gas turbine equipped with a wet compression system and integrated with air-film blade cooling, to address the importance of gas turbine efficiency. The results of the investigated basic and modified cycles present that for a turbine inlet temperature of 1400 °C, an ambient temperature of 45 °C, and relative humidity of 15%, adding an evaporative cooler to a simple gas turbine cycle leads to an approximately 21% increase in specific work, from 331 to 273.7 kJ/kg air, compared to the simple cycle. The exergy analysis indicates that the highest exergy destruction occurs in the combustion chamber, owing to the large temperature differences and the highly irreversible exothermic chemical reactions.

Keywords: Air-film cooling blade; Gas turbine; Wet compression; Energy; Exergy

Introduction

The efficiency of a gas turbine has directly related to its Turbine Injection Temperature (TIT). Therefore, hotter combustion gases can produce more specific power when they are injected into the first turbine stage. The TIT is limited by constraints such as the allowable blade root stress, the creep strain, and the melting point, collectively known as metallurgical limits of the blade material. The density of the blade material can directly affect the stress at the root of blades. Also, this stress increases linearly with both the square of the ratio of the root-to-tip radius and the square of the rotational speed. A rule of thumb regarding the blade life is that for each 10 °C increment in the temperature of the metal (for a specific blade material and cooling technology), the blade life is halved [1]. The centrifugal stresses at the root of blades are expected to increase even more because of the typical high density of nickel-based alloys, materials commonly used for the blades. In this regard, the technology of channeling compressor cold air to cool the turbine blades has attained a more important role in recent years. Utilizing and analyzing different methods associated with this advanced

*First corresponding author: h.athari@sfc.ac.ir
**Second corresponding author: st_m.abdollahihaghi@urmia.ac.ir

cooling technique can be useful in reaching higher TITs beyond the melting point of the blade materials.

For modern engines, normally around 20% of the compressed air is bled off for cooling and sealing purposes of turbine blades and nozzle guide vanes [2]. All the inner walls of the turbine, as well as the disks and turbine rotor blades, can be cooled using the air bleed through their inner passageways. The first stage of stators (or nozzle guide vanes) are exposed to the highest temperatures, including the local hot spots from the combustor close by. The temperature at the first rotor stage is decreased when the gases are diluted with the cooling air, the relative velocity effects, and the power extraction, whereby the gas expansion leads to a drop in its temperature. In the ideal state, the cooling air can be injected at a very low velocity and create a protective cooling film around the blade, known as film cooling. During this process, the temperature reduces along each blade row. Kim [3] assessed a PET/cellulose composite sheet indirect evaporative cooler (IEC) as wetting media and compared it to exiting aluminum and PET IEC and reported that the material change increases the wet-bulb effectiveness by 44%.

The effect of surface modifications and hybrid nanofluids in the regenerative evaporative cooler was appraised by Kashyap et al. [4] from energy-exergy viewpoints. They stated that surface modification follows a significant enhancement in the performance of the regenerative evaporator cooler. An innovative inlet air cooling technology was proposed by Saghafifar and Gadalla [5] for gas turbines employing integrated solid desiccant and also Maisotsenko cooler. They performed transient and economic analyses for inlet air cooling systems and showed that for a 50 MWe gas turbine power plant, with life savings of 31.882 MUS$, the Maisotsenko evaporative desiccant inlet air cooling is the best economic method, in UAE for a book life of 25 years. Salehi et al. [6] assessed gas turbine performance through evaporative cooling via a stage stacking algorithm gambit. They reported that saturated fogging of 1% overspray causes a 24.84% increase in net power output and 6.70% in thermal efficiency, at ambient conditions.

The thermoeconomic features of two basic gas turbine cycles and intercooled gas turbine cycles were investigated by Kumar and Sanjay [7]. They analyzed these cycles as two different gas turbine power utility configurations. Results obtained showed that modified cycle-based power utility delivers about 40% higher plant specific work and requires 47.34% higher fuel during operation. In order to tackle the problem of decreasing gas turbine performance during hot and humid summer periods, when the power demand reaches a maximum, the gas turbine inlet cooling methods can introduce extremely effective solutions. Furthermore, the increasing demands for power output and offsetting shortages during peak load times in hot summer months can be met by utilizing fogging for inlet cooling of gas turbine cycles [8]. Hosseini et al. [9] modeled and evaluated a media evaporative cooling system installed in the gas turbine of Fars combined-cycle power plant (Iran) and showed that by using media evaporative cooling, the output of the gas turbine of the power plant increases by 11 MW at an ambient temperature of 38 °C and relative humidity of 8%, for the inlet air temperature drop of about 19 °C.

The first study on the energy analyses of fogging to achieve a saturated state with 1% and 2% overspray was carried out by Sanaye and Tahani [10]. They found that the drop in the inlet air temperature causes an increase in density and mass flow rate of the inlet air which increases the power input to the compressor. This effect is increased and reaches a maximum when the inlet air is saturated with moisture. The gas turbines, which are essentially constant volume equipment, can convey a certain volume of air at a given shaft speed. However, the power output of a turbine depends directly on the mass flow of the air, which translates to the power output declines on hot days, when air is less dense. The studies show that a 1 °C temperature rise in the inlet air temperature leads to a decrease of 1% in the power output, while the heat rate of the turbine increases at the same time [11]. The numerical result for this type of cycle has been presented by Athari et al. [12], in the form of comparative exergoeconomic analyses of a gas turbine power plant integrated with biomass gasification, with and without fogging inlet cooling. They showed that biomass gasification can be useful in providing clean and efficient power generation. They also reported that a gas turbine cycle with steam injection and fog cooling can be a reasonable alternative within the scope of energy, exergy, and exergoeconomic analyses [13,14].

Many other studies use the fogging cooling method by coupling the gas turbine cycle with environmentally friendly and renewable energy sources such as biomass, a widely available and clean source of energy via the biomass integrated fogging steam injected gas turbine [15–18]. Moreover, the optimum conditions of evaporative cooling for the cycles equipped with steam injection gas turbine was

studied by Fallah et al. [19], using conventional exergy analysis. Kumar and Sanjay [20] investigated the thermoeconomic performance of the air-cooled gas turbine cycle. They determined that the superior cycle in terms of overall cost occurring at a compressor pressure ratio (r_c) of 20 and a turbine inlet temperature of 1500 K. Kumar and Sanjay [21] also focused on the advantages of developing a combined cycle-based power utility.

In the present paper, wet compression integrated with an air-film cooling blade of a gas turbine, through the evaporative system cycle (EVGT) method is studied simultaneously. This cycle can have a decisive role in supplying the energy of small towns and in villages in tropical locations. The main goals of the present paper are to improve understanding and analyzing the performance of the gas turbine cycle. The application of wet compression that is followed by cooling-film blades is investigated from energy and exergy standpoints. Also, parametric studies are carried out to demonstrate the effects of cycle design parameters on the thermodynamic performance of the equipped gas turbine cycle. The obtained results will be beneficial for engineers and designers regarding such systems.

Plant description and assumptions

In this study, evaporative inlet air cooling has been thermodynamically analyzed for performance enhancement of a gas turbine. The designed cycle is shown in **Figure 1**. Ambient air with pressure (P_1), temperature (T_1), and relative humidity (w_1) enters the evaporative cooler. Through passing its media, the air flow's relative humidity reaches 90%, and the air temperature reduces to the corresponding wet-bulb temperature. This process is considered adiabatic mixing. The saturated air is then compressed in the compressor which is characterized by polytropic efficiency up to the desired pressure and then enters the combustion chamber, where the combustion of fuel (CH_4) occurs. In order to limit the maximum temperature of the product gases, which represents the turbine inlet temperature, excess air relative to the stoichiometric air is used, identified by excess air factor. Next, the hot gases expand in the turbine to produce mechanical power, which then produces electrical power in the generator, and is exhausted thereafter.

For the simulation of the gas-turbine cycle, the following are assumed [22]:

- To avoid the influence of the compressor and turbine design specifications (such as type of turbomachinery, total stage number, etc.) on the simulation, the value of the polytropic efficiency is assumed to be fixed and equal to 0.88 in the compressor and the turbine.
- Ambient air is composed of 79% nitrogen and 21% oxygen (volume) and at atmospheric conditions, i.e., P_1=101.325 kPa, T_1=318 K, and φ_{amb}=45%.
- Complete combustion takes place in the combustion chamber under adiabatic conditions, with an efficiency of 99%, and a pressure drop of 4%.
- The fuel consumed in the combustion chamber is methane (CH_4), which has a lower heating value (LHV) of 50,010 kJ/kg.K.

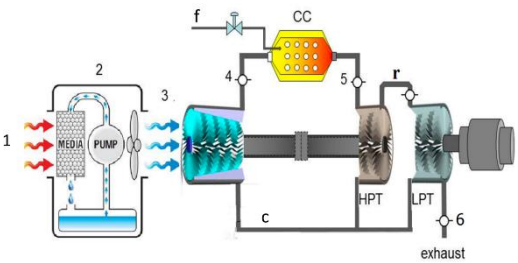

Figure 1 Cooled blade gas turbine cycle with an evaporative cooler.

Modeling

The thermodynamic analysis of the system is performed based on Engineering Equation Solver (EES) software [23]. The program is expedient in developing mathematical models of energy systems and their thermodynamic evaluation.

The cycle is modeled and analyzed by implementing conservation of mass and energy as well as exergy balances for the components of the gas turbine cycle system. The definitions of the mass, energy and exergy balance equations for all components of the system are charted in **Table 1**. The operation parameters (pressure, temperature, enthalpy, entropy) of the corresponding streams of **Figure 1** are tabulated in **Table 1**.

Table 1 Mass, energy and exergy balances equations for the components of the system [24–27].

Comp.	Type	Equations
Evaporator	Mass balance	$m_1 + m_2 = m_3$

	Energy balance	$m_1h_1 + (m_2 - m_1)h_w = m_3h_3$ $\eta_{evaporative\_cooler} = \frac{T_1 - T_2}{T_1 - T_{wb,2}}$
	Exergy balance	$m_1\psi_1 + (m_2 - m_1)\psi_w = m_3\psi_3 + E_{D,evaporative\_cooler}$
Compressor	Mass balance	$m_3 = m_4 + m_c$
	Energy balance	$\int_{T_3}^{T_4} \overline{CP}_{,air} \frac{dT}{T} = \int_{P_3}^{P_4} \frac{\overline{R}}{\eta_{\infty,comp}} \frac{dP}{P}$ $W_{comp} = m_3(h_4 - h_3)$
	Exergy balance	$W_{comp} + m_3\psi_3 = (m_4 + m_c)\psi_4 + E_{D,comp}$
Combustion chamber	Mass balance	$m_4 + m_f = m_5$
	Energy balance	$\int_{298.15}^{T_f} \overline{C}_{P,C_nH_m} dT + \lambda\left(n + \frac{m}{4}\right)\left[\int_{298.15}^{T_4} \overline{C}_{P,O_2} dT + 3.76\int_{298.15}^{T_4} \overline{C}_{P,N_2} dT + 4.76\overline{\omega}_4 \int_{298.15}^{T_4} \overline{C}_{P,H_2O} dT\right] = n\int_{298.15}^{TIT} \overline{C}_{P,CO_2} dT + \left[\lambda\left(n + \frac{m}{4}\right)4.76\overline{\omega}_4 + \frac{m}{2}\right]\int_{298.15}^{TIT} \overline{C}_{P,H_2O} dT + 3.76\lambda(n + m/4)\int_{298.15}^{TIT} \overline{C}_{P,N_2} dT + (\lambda - 1)(n + m/4)\int_{298.15}^{TIT} \overline{C}_{P,O_2} dT - LHV$ $far = \frac{molarmass(C_nH_m)}{\lambda(n + m/4)4.76(1 + m_2)molarmass(air)\eta_{(} - m_c)}$ $x = \frac{n_s \times M_{H_2O}}{\lambda\left(n + \frac{m}{4}\right) \times 4.76 \times (1 + \overline{w}_3) \times M_{air} \times \eta_{cc_3}}$
	Exergy balance	$(m_3 - m_c)\psi_4 + m_f\psi_f = (m_3 - m_c + m_f)\psi_5 + E_{D,cc}$
Turbine	Mass balance	$m_5 + m_c = m_6$
	Energy balance	$\int_{TOT}^{T_r} \overline{C}_{P,g} \frac{dT}{T} = \int_{P_6}^{P_5} \eta_{\infty,turb} \overline{R} \frac{dP}{P}$ $T_r = 0.8451\ TIT + 136.2$ $(m_3 - m_c + m_f)h_5 + \frac{m_c}{2}h_4 = (m_3 - \frac{m_c}{2} + m_f)h_r$ $\frac{h_5 - h_r}{h_5 - h_4} = \frac{m_c}{2m_3 - m_c + 2m_f}$ $W_{turb} = (m_4 + m_f)(h_5 - h_4) + m_c(h_5 - h_3)$
	Exergy balance	$m_c\psi_4 + (m_3 - m_c + m_f)\psi_5 = (m_3 + m_f)\psi_6 + w_{trub} + E_{D,trub}$

In this study, as seen in **Table 1**, n and m are 1 and 4 respectively for CH_4, and the w_3 is specific humidity per a molar of dry air at point 3. The combustion chamber efficiency is denoted by η_{cc} and λ is the excess air fraction. Also, the n_s is the number of moles of steam. Therefore, the value of far (Ratio of fuel mass injected from combustion chamber to the inlet air mass) can be obtained by the equation in this table. The energy efficiency of the cycle is:

$$\eta_{cycle} = \frac{W_{net}}{far \times LHV} \times 100 \quad (1)$$

The exergy analysis is based on the exergy of fuel and exergy of the product. The exergy destruction ratios $y_{D,k}$ given below for the cycle components are charted in **Table 1**. Also, the irreversibility rate for the overall cycle can be evaluated as the sum of the irreversibility rates in each part of the cycle. The second-law efficiency $\eta_{||,cycle}$ is given as:

$$\eta_{||,cycle} = \frac{W_{net}}{m_f \times \psi_{far}} \quad (2)$$

$$y_{D,k} = \frac{E_{D,k}}{E_{D,tot}} \quad (3)$$

In equation 4, $E_{D,tot}$ is the total exergy destruction and can be written as:

$$E_{D,tot} = \sum_{i=1}^{K} E_{D,i} \quad (4)$$

The irreversibility rate in each part of the cycle and for the overall cycle can be evaluated using **Table 1**.

Validation

The thermodynamic properties including temperature, pressure, specific enthalpy, and specific entropy of the streams are tabulated in **Table 2** the validation of the simulated model results from the developed code is carried out by comparing them with reported literature and the results of experimental assessments. More specifically, the results are initially compared with those of Sanaye et al. [9] for different types of turbines in a simple gas turbine cycle utilizing a cooling cycle. This comparison is shown in **Table 3**, where TIT, TOT, η, and $\dot{W}_{net}$ denote respectively turbine inlet temperature, turbine outlet discharge temperature, efficiency, and net power production rate of the cycle.

Table 2 Thermodynamic properties of streams.

Stream	T (K)	P (kPa)	h (kJ/kg)	s (kJ/kg)

1	318.15	101.13	-464.50	7.15
2	298.15	101.13	104.80	0.36
3	312.01	101.13	-466.40	7.08
4	735	1520	-238.50	7.23
5	1530	1440	-2747	9.31
6	910	101.13	-3640	9.48
f	298.15	1200	-4651	10.31
c	735	1520	-238.50	7.23

Table 3 Comparison of computed results with Ref. [9].

Gas Turbine		GE LM2500	GE MS9331	ABB GT10	WH W501D5
Pressure Ratio		18.9	15	14	14.2
Turbine Inlet Temperature (TIT)(°C)		1258	1353	1218	1180
Turbine outlet Temperature (TOT) (°C)	Experimental [9]	532	610	555	535
	This study	601	689	630	615
Efficiency (%)	Experimental [9]	34.6	35	33.3	32.8
	This study	33.53	33.9	31.7	31.13
Specific Net Work (kJ/kg)	Experimental [9]	315	380	315	295
	This study	317	375.3	308.2	289.3

Moreover, the validation of the fogging part of the code was performed using the results obtained by Sanaye and Tahanni [10]. These results are found for the GE917IE turbine on a simple gas turbine cycle with fogging as given in **Table 4**. Note that the abbreviations CIT and CDT stand for compressor inlet temperature and compressor discharge temperature, respectively. As observed, the simulation results are validated as compared with the reference.

Table 4 Comparison of computed results with Ref. [10] for selected conditions (TIT=1122 °C, r_c=11.84, inlet mass rate of turbine=374.59 kg/s).

Parameter	Present study	Ref. [10]
CIT (°C)	30.08	30.00
CDT (°C)	286.9	293
$\dot{W}_{net}$ (MW)	296	283
TOT (°C)	577	553

Results and discussion

The effects of changes in the compressor pressure ratio, relative humidity, and ambient temperature on relative exergy destruction for the compressor are presented in **Figure 2** and **Figure 3**. According to these figures, by increasing the pressure ratio, the relative irreversibility of the compressor increases; this is because of the higher compressor outlet air temperature and its exergy. As observed, the air-film blade cooling phenomena affect the evaporation of water and elicits the irreversibility to decline. Furthermore, increasing either the humidity ratio or the ambient temperature reduces the irreversibility within the compressor.

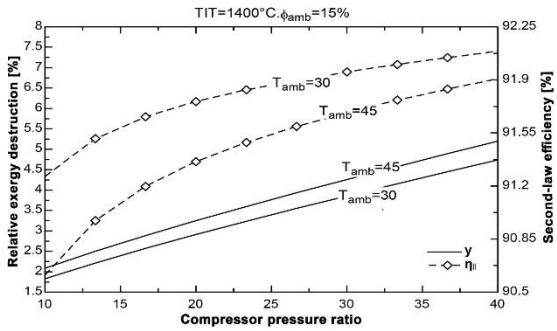

Figure 2 Relative exergy destruction within the compressor and second-law efficiency versus compressor pressure ratio (r_c) at two different ambient temperatures.

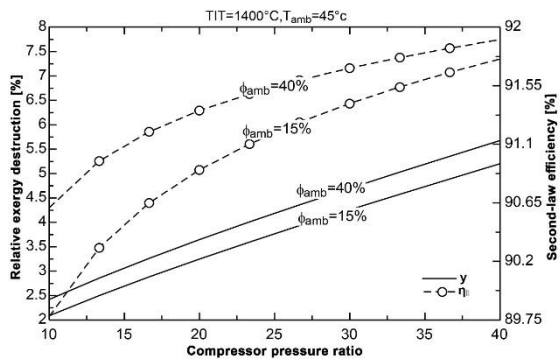

Figure 3 Relative exergy destruction within the compressor and second-law efficiency versus compressor pressure ratio at two ambient humidity.

Also, it is witnessed that the curves are not monotonous in **Figure 2** and **Figure 3**, which is attributable to the fact that the relative exergy destruction of the compressor is directly related to the compressor power consumption, identified as a logarithmic function of the pressure ratio.

Since the largest value of the exergy destruction ratio occurs in the combustion chamber, it is of utmost importance to investigate the effect of changes in inlet conditions on its irreversibility. The relative exergy destruction within the combustion chamber against inlet conditions is demonstrated in **Figure 4** and **Figure 5**. It is observed that by raising the pressure ratio and ambient temperature, the

combustion chamber's irreversibility is reduced. This can again be explained by the higher outlet temperature of the compressor and its exergy associated with a higher pressure ratio, as well as with higher ambient temperature.

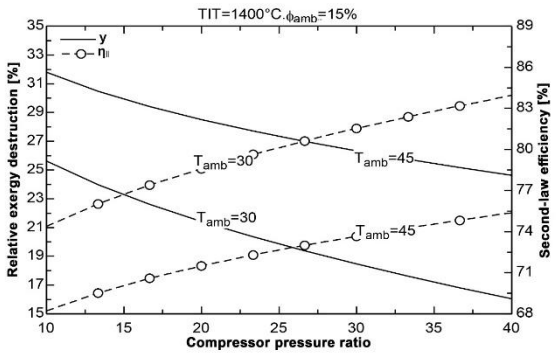

Figure 4 Relative exergy destruction within the combustion chamber and second-law efficiency versus compressor pressure ratio at two different ambient temperatures.

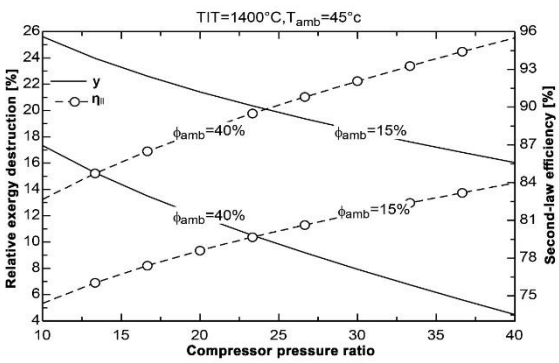

Figure 5 Relative exergy destruction within the combustion chamber and second-law efficiency versus compressor pressure ratio at two ambient humidity.

In **Figure 6**, identical conditions are shown for the turbine. During the wet compression process, a large amount of exergy is recovered, allowing for higher mass flow rates into the turbine. As a major source of irreversibility, the large temperature difference, and several chemical reactions occurring in this component leads to the combustion chamber having the highest exergy destruction among system components.

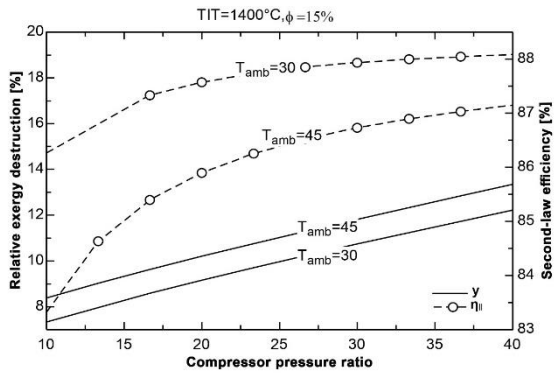

Figure 6 Relative exergy destruction within the turbine and second-law efficiency versus compressor pressure ratio at two different ambient temperatures.

Power output for simple gas turbine cycle with evaporative system cycle (EVGT) and simple gas-turbine system (SGT) against changes in compressor pressure ratio are shown in **Figure 7**. The positive effect of using the evaporative system cycle in a simple gas turbine on power output is readily witnessed. Also, an increase in the ambient temperature is shown to raise the compressor power consumption, causing a reduction in the net power production of both cycles.

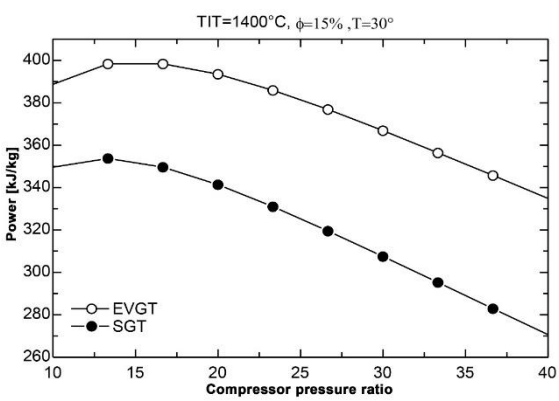

Figure 7 Net power production of the cycle with (EVGT) and without (SGT) evaporator versus compressor pressure ratio.

By scrutinizing **Figure 8** and **Figure 9**, it is seen that in the evaporative cycle, for a fixed pressure ratio, higher ambient temperature leads to higher compressor power consumption, even though the mass flow rate entering the turbine remains almost constant. Another important result of increasing the ambient temperature is that notwithstanding the approximately fixed gross power produced by the

turbine, the net power production of the cycle reduces in higher ambient temperatures. For some ambient temperatures, the net power production and energy and exergy efficiencies of the gas turbine exceed those of the cycle.

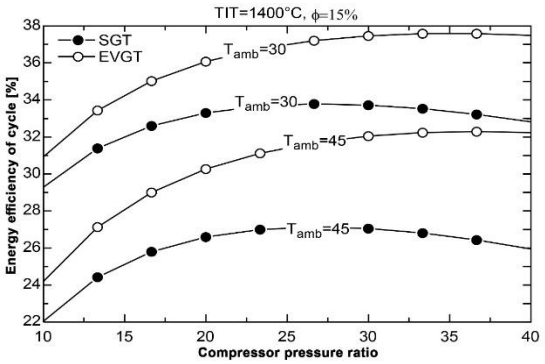

Figure 8 Energy efficiency of EVGT cycle with and without evaporator SGT versus compressor pressure ratio.

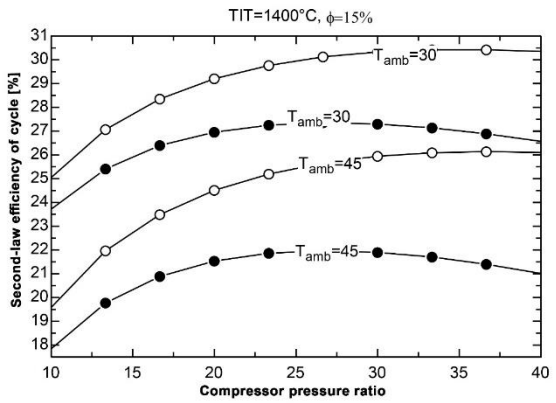

Figure 9 Second-law efficiency of EVGT cycle with and without evaporator SGT vs. compressor pressure ratio.

In the present modified evaporative cycle, the produced power can be increased by raising the total mass flow rate through the turbine. Also, the air-film blade cooling effect results in lower compressor power consumption which in turn yields an increase in net power output. The energy and exergy efficiencies of the gas turbine equipped with the evaporator are maximized at specific values of compressor pressure ratio. Also, increasing the inlet ambient temperature has a stronger effect on the energy and exergy efficiencies of the cycle when there is no evaporator. In addition to this, it is concluded that the maximum output power and energy efficiency of cycles can be found by determining the optimum point of these curves at different arbitrary conditions. The desired pressure ratio of the compressor is charted in **Table 5** and **Table 6**.

Table 5 Maximum output power of cycle in follow conditions (inlet mass flow rate of the cycle is 1 kg/s and φ_{amb}=15%).

T_{amb} (°C)	TIT (°C)	Design Parameter	Type of Cycle	
			SGT	EVGT
30	1100	r_c	8.27	9.4
		far (kg fuel/kg air)	0.018	0.0186
		caf (kg cooling air/kg air)	0.091	0.0923
		Max W_{net} (kJ/kg air)	230.3	260
	1250	r_c	10.44	12.02
		far (kg fuel/kg air)	0.0203	0.0208
		caf (kg cooling air/kg air)	17	0.1331
		Max W_{net} (kJ/kg air)	287.6	325.3
	1400	r_c	12.91	14.93
		far (kg fuel/kg air)	0.0297	0.023
		caf (kg cooling air/kg air)	0.1317	0.1634
		Max W_{net} (kJ/kg air)	353.8	400
45	1100	r_c	9.569	11.33
		far (kg fuel/kg air)	0.017	0.0177
		caf (kg cooling air/kg air)	0.097	0.0984
		Max W_{net} (kJ/kg air)	160	195
	1250	rc	12.14	14.4
		far (kg fuel/kg air)	0.019	0.1998
		caf (kg cooling air/kg air)	0.139	0.1406
		Max W_{net} (kJ/kg air)	209.7	257
	1400	r_c	15.11	18
		far (kg fuel/kg air)	0.0216	0.0223
		caf (kg cooling air/kg air)	0.1696	0.1718
		Max W_{net} (kJ/kg air)	273.7	331

Table 6 Maximum energy efficiency of the cycle in follow conditions (inlet mass flow rate of the cycle is 1 kg/s and φ_{amb}=15%).

T_{amb} (°C)	TIT (°C)	Design parameter	Cycle	
			SGT	EVGT
30	1100	r_c	14.3	17.83
		far (kg fuel/kg air)	0.0158	0.0157
		caf (kg cooling air/kg air)	0.1023	0.1052
		Max μ_{cycle} (%)	26.93	30.6
	1250	r_c	19.78	25.14
		far (kg fuel/kg air)	0.0173	0.0172
		caf (kg cooling air/kg air)	0.142	0.152

		Max μ_{cycle} (%)	30.32	33.83
	1400	r_c	27.11	35.18
		far (kg fuel/kg air)	0.018	0.0186
		caf (kg cooling air/kg air)	0.1843	0.1893
		Max μ_{cycle} (%)	33.78	37.67
45	1100	r_c	13.84	18.05
		far (kg fuel/kg air)	0.015	0.0154
		caf (kg cooling air/kg air)	0.1054	0.1087
		Max μ_{cycle} (%)	18.91	23.15
	1250	r_c	19.38	25.83
		far (kg fuel/kg air)	0.0169	0.016
		caf (kg cooling air/kg air)	0.1527	0.157
		Max μ_{cycle} (%)	23.00	27.8
	1400	r_c	26.93	36.89
		far (kg fuel/kg air)	0.018	0.018
		caf (kg cooling air/kg air)	0.189	0.195
		Max μ_{cycle} (%)	27.13	32.4

As seen in **Figure 10** and **Figure 11**, caf increases by increasing the ambient temperature, relative humidity, or pressure ratio. A reduction in far means an increase in caf. This can be explained by pointing out that by reducing the fuel consumption (in order to achieve the specified TIT), the amount of air entering the combustion chamber also lowers. This is based on the assumption of constant air mass flow in the inlet cycle (1 kg). This reduction can be translated as a higher ratio of the air being used for blade cooling.

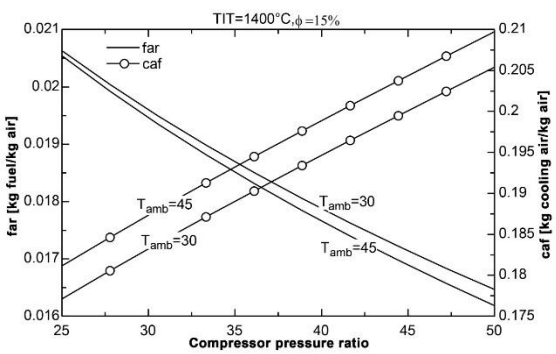

Figure 10 The value of far and caf in EVGT cycle versus compressor pressure ratio at different ambient temperature.

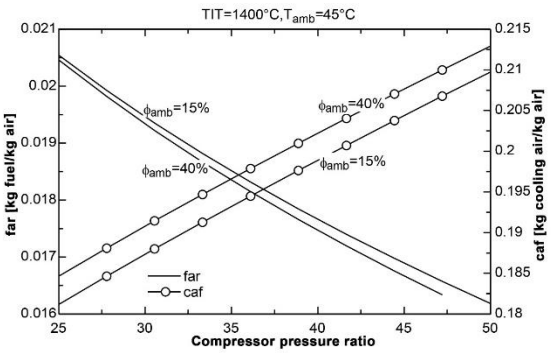

Figure 11 The value of far and caf in EVGT cycle versus compressor pressure ratio at different air humidity.

Conclusions

Utilizing an evaporator for inlet cooling of gas turbine cycles is shown to be a promising method to improve the gas turbine performance, which is of paramount importance in meeting the ever-increasing demands for power as well as offsetting shortages during peak load periods, especially in the summertime. This paper studied the maximum output power, energy, and exergy efficiencies of the standard gas turbine cycles with and without evaporative cooling and determined the optimum condition for different arbitrary conditions.

For the studied cycles in this paper, the results show that the maximum output power is obtained for the EVGT cycle at the following conditions: TIT=1400 K, T_{amb}=30, r_c =14.93, FAR=0.023 (kg fuel/kg air), and CAF=0.1634 (kg cooling air/kg air). The maximum energy and exergy efficiencies can also be found by the same method. The following conclusions are drawn from the results:

- An EVGT is superior to the simple SGT cycle considered in terms of power output, energy, and exergy efficiencies.
- For systems with and without the evaporator, the variations of calculated values of generated power show that for the case of inlet cooling, the net power slightly decreases when air temperature and air relative humidity are increased for both cycles.
- The modeling and analyses of the wet compression processes, which were verified by comparing with corresponding data reported in the literature, demonstrate the potential of wet compression for decreasing the compressor inlet air temperature for various ambient conditions (temperature and relative humidity).
- The effects of wet compression in the compressor on power output and exergy efficiency for gas-

turbine cycles are investigated based on compressor pressure ratio (rc) and two parameters of ambient temperature and humidity.

- The analysis of all components of the EVGT cycle showed that the largest irreversibility rate is related to the combustion chamber, whereby the large temperature differences for heat transfer and highly exothermic chemical reactions significantly increase the irreversibility. Also, the exergy efficiencies of the gas turbine cycle are compared at the maximum power conditions, for various values of ambient temperature and humidity.
- For a simple gas-turbine system, wet cooling can improve the power output as well as the energy and exergy efficiencies. Increasing the TIT increases the energy and exergy efficiencies in the EVGT plant, and a higher TIT usually necessitates the utilization of air-film blade cooling blades technology.
- In terms of power output and utilization of the maximum inlet turbine temperature, a gas turbine cycle with a media-type evaporator and inter-cooling blades is more advantageous compared to the other cycles considered.

Nomenclature	
CIT	Compressor inlet temperature (°C)
CDT	Compressor discharge temperature (°C)
caf	Ratio of cooling air mass to inlet air mass
E	Exergy (kJ)
EVGT	Gas turbine cycle with evaporator cooler
far	Ratio of fuel mass to inlet air mass
h	Specific enthalpy (kJ/kg)
h_a	Specific enthalpy of dry air (kJ/kg)
h_v	Specific enthalpy of vapor (kJ/kg)
$\dot{m}_a$	Mass flow rate of dry air (kg/s)
$\dot{m}_i$	Mass flow rate of steam at location i (kg/s)
$\dot{m}_f$	Mass flow rate of the absorbed water in evaporator cooler (kg/s)
$\dot{m}_w$	Mass flow rate of unevaporated water (overspray) in fogging cooler (kg/s)
$\dot{m}_{fuel}$	Mass consumption rate of fuel in cycle (kg/s)
$\dot{m}_s$	Mass flow rate of steam injected into combustion chamber (kg/s)
n_s	Molar quantity of steam (mole)
r_c	compressor pressure ratio
s	Specific entropy (kJ/kg. K)
SGT	Simple gas turbine cycle without fogging system
TIT	Turbine inlet temperature (°C)
TOT	Turbine outlet temperature (°C)
w	Specific humidity
$\overline{w}_i$	Specific humidity per 1 molar of dry air at point i
W	Power (kJ)
$\dot{W}_{turb}$	Outlet power of turbine (kW)
X	Ratio of injected steam from heat recovery steam generator to 20 kg inlet air mass
Greek Letters	
ε	Exergy efficiency (%)
η	Energy efficiency (%)
ψ_i	Specific exergy of steam at location i (kJ/kg)
ψ_s	Specific exergy of steam injected into combustion chamber (kJ/kg)
ψ_f	Specific exergy of sprayed water in fogging cooler (kJ/kg)
ψ_w	Specific exergy of unevaporated water (overspray) (kJ/kg)
ψ_{fuel}	Specific exergy of fuel consumed in cycle (kJ/kg)
ψ_{stack}	Specific exergy of outlet gases from stack (kJ/kg)
λ	Excess air fraction
Subscripts	
CC	Combustion chamber
Ch	Chemical
Comp	Compressor
D	Destruction
F	Fogging
HRSG	Heat recovery steam generator
i	State point
Mix	Mixture
Ph	Physical
S	Steam
Turb	Turbine
W	Water

References

[1] Rolls Royce. The Jet Engine. Wiley; 5th edition; 2015.

[2] Bassily AM. Performance improvements of the intercooled reheat recuperated gas-turbine cycle using absorption inlet-cooling and evaporative after-cooling. Appl Energy 2004;77:249–72. https://doi.org/10.1016/s0306-2619(03)00099-0.

[3] Kim NH. Performance of an indirect evaporative cooler (IEC) made of PET/cellulose composite sheet as wetting media. Appl Therm Eng 2021;186:116492. https://doi.org/10.1016/j.applthermaleng.2020.116492

[4] Kashyap S, Sarkar J, Kumar A. Effect of surface modifications and using hybrid nanofluids on energy-exergy performance of regenerative evaporative cooler. Build Environ 2021;189:107507. https://doi.org/10.1016/j.buildenv.2020.107507.

[5] Saghafifar M, Gadalla M. Innovative inlet air cooling technology for gas turbine power plants using integrated solid desiccant and Maisotsenko cooler. Energy 2015;87:663–77. https://doi.org/10.1016/j.energy.2015.05.035.

[6] Salehi M, Eivazi H, Tahani M, Masdari M. Analysis and prediction of gas turbine performance with evaporative cooling processes by developing a stage stacking algorithm. J Clean Prod 2020;277:122666.

https://doi.org/10.1016/j.jclepro.2020.122666.

[7] Sahu MK, Sanjay. Thermoeconomic investigation of basic and intercooled gas turbine based power utilities incorporating air-film blade cooling. J Clean Prod 2018;170:842–56. https://doi.org/10.1016/j.jclepro.2017.09.030.

[8] Ehyaei MA, Mozafari A, Alibiglou MH. Exergy, economic & environmental (3E) analysis of inlet fogging for gas turbine power plant. Energy 2011. https://doi.org/10.1016/j.energy.2011.10.011.

[9] Hosseini R, Beshkani A, Soltani M. Performance improvement of gas turbines of Fars (Iran) combined cycle power plant by intake air cooling using a media evaporative cooler. Energy Convers Manag 2007;48:1055–64. https://doi.org/10.1016/j.enconman.2006.10.015.

[10] Sanaye S, Tahani M. Analysis of gas turbine operating parameters with inlet fogging and wet compression processes. Appl Therm Eng 2010;30:234–44. https://doi.org/10.1016/j.applthermaleng.2009.08.011

[11] Kim KH, Ko HJ, Blanco HP. Exergy analysis of gas-turbine systems with high fogging compression. Int J Exergy 2011;8:16. https://doi.org/10.1504/ijex.2011.037212.

[12] Athari H, Soltani S, Rosen M, Mahmoudi S, Morosuk T. Comparative Exergoeconomic Analyses of Gas Turbine Steam Injection Cycles with and without Fogging Inlet Cooling. Sustainability 2015;7:12236–57. https://doi.org/10.3390/su70912236.

[13] Athari H, Soltani S, Bölükbaşi A, Rosen MA, Morosuk T. Comparative exergoeconomic analyses of the integration of biomass gasification and a gas turbine power plant with and without fogging inlet cooling. Renew Energy 2015;76:394–400. https://doi.org/10.1016/j.renene.2014.11.064.

[14] Athari H, Soltani S, Rosen MA, Seyed Mahmoudi SM, Morosuk T. Gas turbine steam injection and combined power cycles using fog inlet cooling and biomass fuel: A thermodynamic assessment. Renew Energy 2016;92:95–103. https://doi.org/10.1016/j.renene.2016.01.097.

[15] Pascale A De, Melino F, Morini M. Analysis of Inlet Air Cooling for IGCC Power Augmentation. Energy Procedia 2014;45:1265–74. https://doi.org/10.1016/j.egypro.2014.01.132.

[16] Kim KH, Perez-Blanco H. Potential of regenerative gas-turbine systems with high fogging compression. Appl Energy 2007;84:16–28. https://doi.org/10.1016/j.apenergy.2006.04.008.

[17] Mahto D, Pal S. Thermodynamics and thermo-economic analysis of simple combined cycle with inlet fogging. Appl Therm Eng 2013;51:413–24. https://doi.org/10.1016/j.applthermaleng.2012.09.003

[18] Ehyaei MA, Tahani M, Ahmadi P, Esfandiari M. Optimization of fog inlet air cooling system for combined cycle power plants using genetic algorithm. Appl Therm Eng 2015;76:449–61. https://doi.org/10.1016/j.applthermaleng.2014.11.032

[19] Fallah M, Siyahi H, Ghiasi RA, Mahmoudi SMS, Yari M, Rosen MA. Comparison of different gas turbine cycles and advanced exergy analysis of the most effective. Energy 2016;116:701–15. https://doi.org/10.1016/j.energy.2016.10.009.

[20] Sahu MK, Sanjay. Investigation of the effect of air film blade cooling on thermoeconomics of gas turbine based power plant cycle. Energy 2016;115:1320–30. https://doi.org/10.1016/j.energy.2016.09.069.

[21] Sahu MK, Sanjay. Comparative exergoeconomics of power utilities: Air-cooled gas turbine cycle and combined cycle configurations. Energy 2017;139:42–51. https://doi.org/10.1016/j.energy.2017.07.131.

[22] Khan JR, Wang T. Fog and Overspray Cooling for Gas Turbine Systems With Low Calorific Value Fuels. Vol. 4 Cycle Innov. Electr. Power Ind. Cogener. Manuf. Mater. Metall., ASMEDC; 2006. https://doi.org/10.1115/gt2006-90396.

[23] EES (Engineering Equation Solver), Version V7.847 n.d.

[24] Delpisheh M, Abdollahi Haghghi M, Mehrpooya M, Chitsaz A, Athari H. Design and financial parametric assessment and optimization of a novel solar-driven freshwater and hydrogen cogeneration system with thermal energy storage. Sustain Energy Technol Assessments 2021;45:101096. https://doi.org/10.1016/j.seta.2021.101096.

[25] Delpisheh M, Haghghi MA, Athari H, Mehrpooya M. Desalinated water and hydrogen generation from seawater via a desalination unit and a low temperature electrolysis using a novel solar-based setup. Int J Hydrogen Energy 2021;46:7211–29. https://doi.org/10.1016/j.ijhydene.2020.11.215.

[26] Cao Y, Mohamed AM, Dahari M, Delpisheh M, Haghghi MA. Performance enhancement and multi-objective optimization of a solar-driven setup with storage process using an innovative modification. J Energy Storage 2020;32. https://doi.org/10.1016/j.est.2020.101956.

[27] Cao Y, Dhahad HA, Sun Y-L, Abdollahi Haghghi M, Delpisheh M, Athari H, et al. The role of input gas species to the cathode in the oxygen-ion conducting and proton conducting solid oxide fuel cells and their applications: Comparative 4E analysis. Int J Hydrogen Energy 2021. https://doi.org/https://doi.org/10.1016/j.ijhydene.2021.03.111.